

Metal–Metal and Carbon–Carbon Bonds as Potential Components of Molecular Batteries

Carlo Floriani,^{*,[a]} Euro Solari,^[a] Federico Franceschi,^[a] Rosario Scopelliti,^[a] Paola Belanzoni,^[a] and Marzio Rosi^[b]

Abstract: The reductive coupling of [M(salophen)] derivatives, where M is an early transition metal and salophen is *N,N'*-*o*-phenylenebis(salicylideneaminate) dianion, led to the formation of dimers linked through C–C and M–M bonds. Both of these bonds can potentially function as electron reservoirs: each bond can be used as a reversible source of a pair of electrons under the condition that it is not chemically transformed by the incoming substrate which functions as an electron acceptor. To explore this potential function as well as the competition in the redox processes between C–C and M–M bonds within the same molecular framework, we investigated the reduction of [(*t*Bu₄-salophen)NbCl₃] (**1**) and [(*t*Bu₄-salophen)MoCl₂] (**7**) as model compounds.

In the former case, the reduction led to [(Nb–Nb)(*t*Bu₄-salophen₂*)] (**2**) which contains both a Nb–Nb bond (2.6528(7) Å) and two C–C bonds across two imino groups of the ligand. Complex **2** can be reduced further to a transient compound **5** that contains an Nb=Nb bond. In the second case, the reduction of **7** by two electrons led to [(Mo≡Mo)(*t*Bu₄-salophen)₂] (**8**), which does not contain any C–C linkages between the two salophen units. Complexes **2** and **5** are able to transfer one

pair and two pairs of electrons, respectively, to give compounds **3**, **4**, and **6**, with the consequent cleavage of the Nb–Nb and Nb=Nb bonds. In the present case, it is surprising that the C–C bonds do not participate in the reduction of the substrates. A careful theoretical treatment anticipates, both in the case of **1** and **7**, the preferential formation of metal–metal bonds upon reduction. This is indeed the case for **7**, but not for **1**, where the formation of C–C bonds competes with that of M–M bonds, the latter being the first ones, however, to be involved in electron-transfer reactions. The theoretical approach allowed us to investigate the possibility of intramolecular electron transfer from C–C bonds to M–M bonds and vice versa.

Keywords: electron reservoirs • metal–metal bonds • molecular batteries • molybdenum • niobium

Introduction

The use of a chemical bond across two atoms for the storage and subsequent release of a pair of electrons seems to be quite an obvious concept. The reductive or oxidative coupling and the reverse decoupling can be the mechanism through which we must pass through.^[1] Many mechanisms are known which operate in at least one direction,^[2, 3] while very often the reverse process does not even occur. Among the very few systems that exhibit reactions in both directions, we should mention the oxidation of organic sulfides to the corresponding disulfide and the reverse reduction.^[4] In addition, such a redox

reaction has relevance in naturally occurring systems.^[5] A major question is under which conditions can we take advantage of a simple chemical bond for storing and releasing electrons.

The major unquestionable goal is the facile reversibility associated with no overall change when the chemical system is returned to its original state. This is a normal event when the redox reactions involving formation and cleavage of a chemical bond are performed electrochemically.^[6] However, reversibility to the original state is much more rarely observed when the redox system is involved in the exchange of electrons with chemical substrates.^[7] As a matter of fact, the exchange of electrons with the substrate usually occurs at centres which function as electron reservoirs, so that the substrate remains bonded to them.^[1, 8]

With the perspective of the use of chemical bonds as electron reservoirs, we selected metal–metal^[3] and carbon–carbon^[2] bonds and we tried to put them in competition within the same molecular framework. Both of them have a quite well-known redox chemistry, though neither of them satisfies completely the requirements mentioned above. This work was

[a] Prof. Dr. C. Floriani, Dr. E. Solari, Dr. F. Franceschi, Dr. R. Scopelliti, Dr. P. Belanzoni
Institut de Chimie Minérale et Analytique
Université de Lausanne, BCH, 1015 Lausanne (Switzerland)
Fax: (+41) 21-692-39-05
E-mail: carlo.floriani@icma.unil.ch

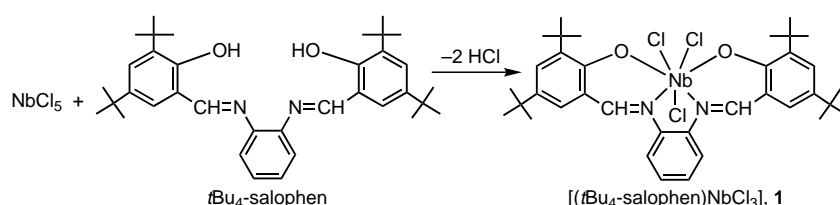
[b] Prof. Dr. M. Rosi
CSCISM, c/o Dipartimento di Chimica
Università di Perugia, 06123 Perugia (Italy)

inspired by our previous discovery that the formation and cleavage of C–C single bonds can be effectively used for storing and releasing a pair of electrons. The model compounds used were a variety of $[M(\text{salophen})]^{9]}$ [salophen = N,N' -*o*-phenylenebis(salicylideneaminato) dianion] or $[M(\text{tmtaa})]^{10]}$ [tmtaa = dibenzotetramethyltetraaza[14]annulene dianion] complexes, which undergo reductive coupling of one or both imino groups to form a C–C bond which is oxidatively broken without the carbon being involved in any chemical transformation. The assistance of a metal centre is compulsory,^{9d, 11]} though it should not display any redox chemistry, as in the case of main-group metals.

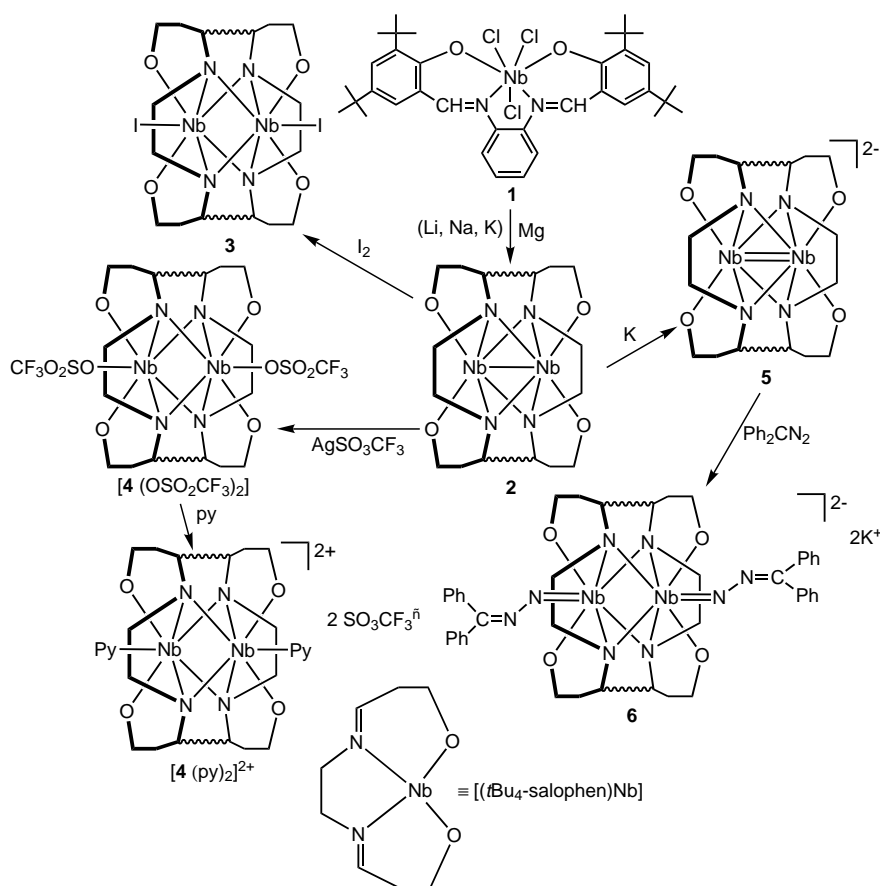
We report here on the redox chemistry of $[\text{Nb}(\text{tBu}_4\text{-salophen})\text{Cl}_3]$ and $[\text{Mo}(\text{tBu}_4\text{-salophen})\text{Cl}_2]$, which undergo reductive coupling to form dimers that contain both C–C and M–M bonds. The experimental results led us to estimate the relative suitability of the two kinds of bonds to act as electron reservoirs, while a full theoretical investigation gave us the possibility to estimate the preferential storage sites of the pair of electrons in the reduction of $[\text{Nb}(\text{salophen})]$ and $[\text{Mo}(\text{salophen})]$ moieties.

Results and Discussion

Chemical studies: The starting material, **1**, was prepared by directly reacting NbCl_5 with the protic form of the Schiff base ligand (Scheme 1) in toluene. This is a high-yield synthesis. In the present case, it would seem wiser to start from a lower oxidation state of the metal, namely from NbCl_4 . In the latter case, the synthesis would have to be carried out by the addition of NbCl_4 to the sodium salt of the *t*Bu-salophenH₂ ligand. However, to free the final Nb complex from NaCl requires a long liquid/solid extraction procedure that leads to lower yields. The three-electron reduction of **1** with alkali metals or, equally well, magnesium, gave the coupled dimer **2** (Scheme 2) that contains two C–C bonds across two Schiff base ligands and a single Nb–Nb bond. The reaction occurs with the simultaneous reduction of the salophen-type ligand



Scheme 1. Synthesis of **1**.



Scheme 2. Redox chemistry of **1** (the dinucleating ligand in **2**–**6** is drawn as doubly C–C-bonded salophen units).

in the usual manner,^{9]} and the reduction of Nb^V to Nb^{IV} . The use of lower molar ratios of Nb:reducing agent only led to a mixture of compounds including **2**, rather than to other less reduced forms. The diamagnetism of the dinuclear complex **2** supports the presence of a single Nb–Nb bond. The dimeric structure of **2** was confirmed by an X-ray structural analysis (Figure 1, Table 1).

The dinucleating ligand [$^*\text{salophen}^*_2$]⁸⁻ (Figure 2), derived from the reductive coupling of two salophen units (C–C 1.628(5) Å) binds the two metal ions, which experience the same coordination environment in a close proximity (Nb–Nb 2.6528(7) Å). The rather short metal–metal single bond length is imposed by the geometric constraints of the dinucleating ligand. The four nitrogen atoms and the four oxygen atoms define two perpendicular planes (99.9°) (Figure 3); the metals lie out of these planes by ± 1.3262 Å and ± 0.2072 Å, respectively.

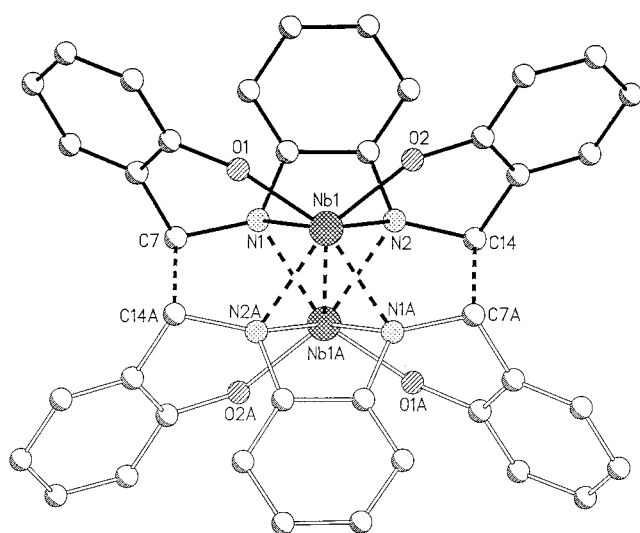


Figure 1. Structure of **2** (hydrogen atoms, solvent molecules, and *t*Bu groups omitted for clarity). Atoms with an "A" indicate the following symmetry transformation: $-x, -y, -z$.

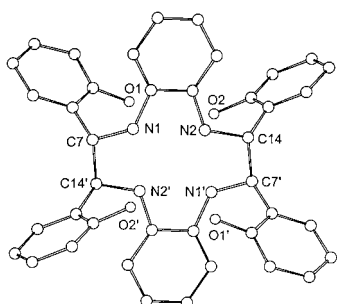


Figure 2. Structure of the $[\text{*salophen}_2\text{*}]^{8-}$ ligand. The *t*Bu substituents are omitted.

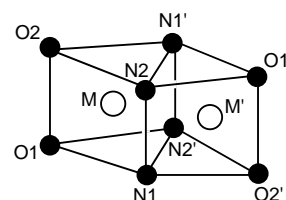


Figure 3. Coordination polyhedra around niobium in complex **2**.

Complex **2** is a potential six-electron reservoir: two of the three pairs of electrons being stored in the two new C–C bonds and the third pair in the Nb–Nb bond. The chemical utilisation of the six electrons was attempted by the reaction of **2** with reducible substrates. The reaction of **2** with iodine led to the cleavage of one of the three single bonds, namely Nb–Nb, to give the diamagnetic complex **3** (Scheme 2). The structure of complex **3**, formed by the preferential cleavage of the metal–metal bond, while the two C–C bonds remain intact, is supported by the analogous reaction of **2** with AgSO_3CF_3 . In the latter case, the reduction of Ag^+ to elemental Ag occurs along with the cleavage of the metal–metal bond, while the two C–C bonds do not participate in the electron-transfer reaction. The reaction led to the formation of a dication **4** with weakly bonded triflate counteranions. They are readily displaced by pyridine, leading to the bis-pyridine derivative $[\mathbf{4}(\text{Py})_2][\{\text{SO}_3\text{CF}_3\}_2]$. Figure 4 displays the structure of the dication **4**.

The structure of **4** is quite reminiscent of that of **2**. The metal ions maintain the same coordination environment, except for the greater separation between the Nb atoms ($2.793(2)$ Å). This separation, which is almost a bonding distance, is an artifact imposed by the binucleating nature of the ligand. The structural parameters of the ligand and the

Table 1. Crystal data and details of the structure determination of **2**, **4**, **6** and **8**.

	2	4	6	8
chemical formula	$\text{C}_{80}\text{H}_{108}\text{N}_4\text{Nb}_2\text{O}_6 \cdot 4\text{C}_4\text{H}_8\text{O}$	$\text{C}_{82}\text{H}_{102}\text{N}_6\text{Nb}_2\text{O}_4 \cdot 2\text{C}_5\text{H}_5\text{N} \cdot 2\text{CF}_3\text{O}_3\text{S}$	$\text{C}_{110}\text{H}_{140}\text{K}_2\text{N}_8\text{Nb}_2\text{O}_{10} \cdot 4\text{C}_4\text{H}_8\text{O}$	$\text{C}_{72}\text{H}_{92}\text{Mo}_2\text{N}_4\text{O}_4 \cdot 0.5\text{C}_7\text{H}_{16}$
formula weight	1695.94	1877.86	2286.74	1319.47
crystal system	triclinic	monoclinic	monoclinic	monoclinic
space group	$\bar{P}1$	$C2/c$	$P2_1/n$	$P2_1/n$
<i>a</i> [Å]	11.4000(8)	33.7400(9)	15.580(3)	14.978(2)
<i>b</i> [Å]	14.6516(16)	14.6600(4)	21.308(4)	20.702(3)
<i>c</i> [Å]	15.7605(16)	19.3800(5)	19.578(5)	23.268(3)
α [°]	67.138(10)	90	90	90
β [°]	70.013(8)	99.2600(12)	113.18(2)	104.657(12)
γ [°]	89.516(7)	90	90	90
<i>V</i> [Å ³]	2255.9(4)	9461.0(4)	5975(2)	6980.3(17)
<i>Z</i>	1	4	2	4
ρ_{calcd} [g cm ⁻³]	1.248	1.318	1.271	1.256
<i>F</i> (000)	906	3920	2432	2788
μ [mm ⁻¹]	0.313	0.358	0.326	0.409
<i>T</i> [K]	143	143	143	173
λ [Å]	0.71073	0.71070	0.71070	0.71073
measured reflections	13 709	25 577	31 162	39 485
unique reflections	6808	6365	9161	11 625
unique reflections [$I > 2\sigma(I)$]	5559	3718	5937	9459
data/parameters	6808/506	6365/538	9161/686	11 625/794
<i>R</i> ^[a] [$I > 2\sigma(I)$]	0.0532	0.1085	0.0561	0.0725
<i>wR</i> ^[a] (all data)	0.1321	0.3493	0.1566	0.1638
GoF ^[b]	1.110	1.107	0.950	1.174

[a] $R = \sum ||F_o| - F_c| / \sum |F_o|$, $wR2 = [\sum [w(F_o^2 - F_c^2)]^2 / \sum [w(F_o^2)]^2]^{1/2}$. [b] $\text{GoF} = [\sum [w(F_o^2 - F_c^2)] / (n - p)]^{1/2}$ where *n* is the number of data and *p* is the number of parameters refined.

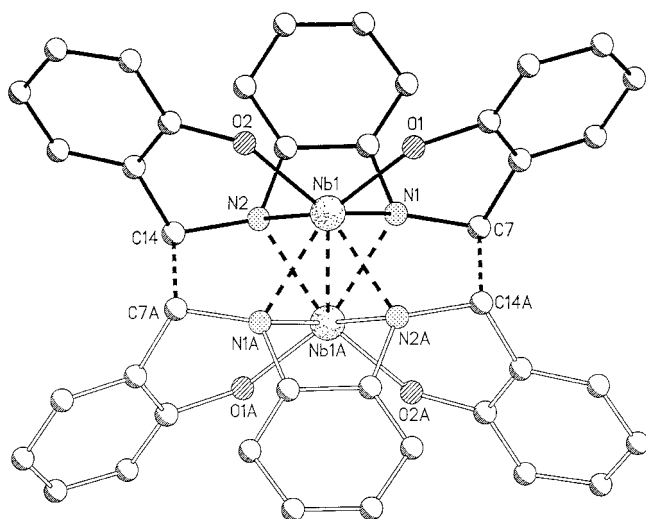


Figure 4. Structure of **4** (hydrogen atoms, CF_3SO_3^- , solvent molecules, and *t*Bu groups omitted for clarity). Atoms with an "A" indicate the following symmetry transformation: $-x + 1/2, -y + 1/2, -z$.

coordination sphere of the metal (Nb– N_{av} 2.183(10); Nb– O_{av} 1.963(8) Å) (see Table 2) are very close to those of **2**. The four oxygen atoms and the four nitrogen atoms define two planes which are almost perpendicular to each other (79.5°). The Nb atoms are displaced from those planes by ± 1.3963 and ± 0.2334 Å, respectively.

Table 2. Selected bond lengths [Å] and angles [$^\circ$] for complexes **2**, **4**, **6** and **8**.

	2	4	6	8
M–O1 ^[a]	2.034(3)	1.955(8)	2.003(3)	2.047(4) [2.061(4)] ^[c]
M–O2 ^[a]	2.027(3)	1.971(8)	1.981(3)	2.060(4) [2.047(4)] ^[c]
M–N1 ^[a]	2.159(3)	2.157(10)	2.315(4)	2.116(4) [2.109(4)] ^[c]
M–N2 ^[a]	2.157(3)	2.188(10)	–	2.118(5) [2.119(4)] ^[c]
M–N1A ^[a]	2.182(3)	2.211(10)	2.234(4)	–
M–N2A ^[a]	2.185(3)	2.177(10)	2.080(4)	–
M–L ^[a, b]	2.312(3)	2.279(10)	1.820(4)	–
M...M ^[a]	2.6528(7)	2.793(2)	3.4214(11)	2.2057(8)
C–C ^[d]	1.628(5)	1.591(17)	1.605(6)	–
N3–N4	–	–	1.357(5)	–

[a] M = Nb (**2**, **4** and **6**), M = Mo (**8**). [b] L = THF (**2**), L = Pyr (**4**), L = Ph_2CN_2 (**6**). [c] Values in brackets refer to the second Mo (hence Mo2, O3, O4, N3, N4). [d] Values corresponding to the carbon single bond linking the two ligands.

There are some aspects of this chemistry which are rather intriguing. One of them is the oxidative resistance of the C–C bonds: in all the other cases previously reported,^[9] they are very sensitive to cleavage by any kind of oxidising agent. The cleavage of C–C bonds by iodine in other coupled [M(salophen)] complexes is well documented.^[9b] In addition, we did not succeed in cleaving the C–C bond, even by the use of stronger oxidising agents, including dioxygen. In the latter case, the formation of a mixture of different compounds was observed. According to the theoretical calculations reported in the next section, the Nb–Nb bond is much more stable and stronger than the C–C bonds. This notwithstanding (see also below), the metal–metal bonds are the first ones to cleave upon oxidation. This is probably not in conflict with the

theoretical results. The reaction leads, very probably, to the kinetic product which does remain stable in a metastable form. In fact, we found that the HOMO orbitals available to the oxidising agents were always localised on the metal centres, so that the electrons flow from the real reservoir, namely the C–C bonds, to the metal in the reduction of the substrates.^[9d, 11] We expected, however, an intramolecular transfer of a pair of electrons from the C–C bond to the metal, with the overall cleavage of a C–C bond and the formation of a Nb–Nb bond.

In this context (see the next section), we should also mention that the existence of **2** is not predictable on the basis of pure calculations. The corresponding isoelectronic systems that contain a Nb≡Nb bond and no C–C bond are, as a matter of fact, foreseen as much more stable. The further reductions of **2** were expected to produce stable compounds of Nb^{III}-d² and Nb^{II}-d³ containing an Nb=Nb and an Nb≡Nb functionality, respectively. In the case of the two-electron reduction of **2**, we were unable to isolate **5**, although we succeeded in intercepting it in the presence of an appropriate substrate. The reduction of **2** with two equivalents of potassium metal was carried out in the presence of diphenyldiazomethane. The reaction led to the formation of a dimetallic diphenylhydrazone dianion (**6**; Scheme 2). The formation of **6** requires the intermediate formation of **5**, in which the Nb=Nb bond functions as a four-electron reservoir for the reduction of two molecules of Ph_2CN_2 . There is a close analogy in the chemical behaviour of this Nb=Nb bond with that reported in calix[4]arene–niobium(III) chemistry,^[12] where the metal–metal double bond was able to perform the four-electron reduction of dinitrogen,^[12d] ketones^[12a] and carbon monoxide.^[12c] Under the present experimental conditions, it is quite difficult to find other substrates that are able to intercept the [Nb=Nb] reactive functionality without reacting with potassium metal in a preliminary stage.

Complex **6** is also a dimetallic compound, in which the two metal ions are positioned inside the dinucleating ligand (Figure 2 and Figure 5a). Although the ligands maintain the overall topology defined by the N_4 and O_4 planes being perpendicular to each other (99.6°), from which the metal ions are displaced ± 1.5624 Å and ± 0.6790 Å, significant structural changes are observed, mainly in the coordination sphere of the niobium ions, on account of the novel functionalisation of the metal. The two metals are further apart (3.4214(11) Å) than in **2** and **4**, and they are no longer equally distant from the four nitrogen atoms of the N_4 plane. Two of the N atoms function as binding donor atoms shared by the two metal ions. The structural parameters (Table 2) are in agreement with the binding sequence shown in Scheme 2 for the metalla-hydrazone functionality (Nb1–N3 1.820(4), N3–N4 1.357(5), N4–C37 1.312(5) Å). A strong association occurs between the K cations and the basic nitrogens of the hydrazone unit (K1–N3 2.943(4), K1–N4 2.834(4) Å, Figure 5b). The results reported above show that, while the coupling of the imino groups and the metal–metal formation can be in competition upon reduction of **1**, the oxidative decoupling mainly concerns the metal–metal functionality. This finding is not quite what we expected from the theoretical calculations (see below), which are in favor of a much higher stability of the M–M

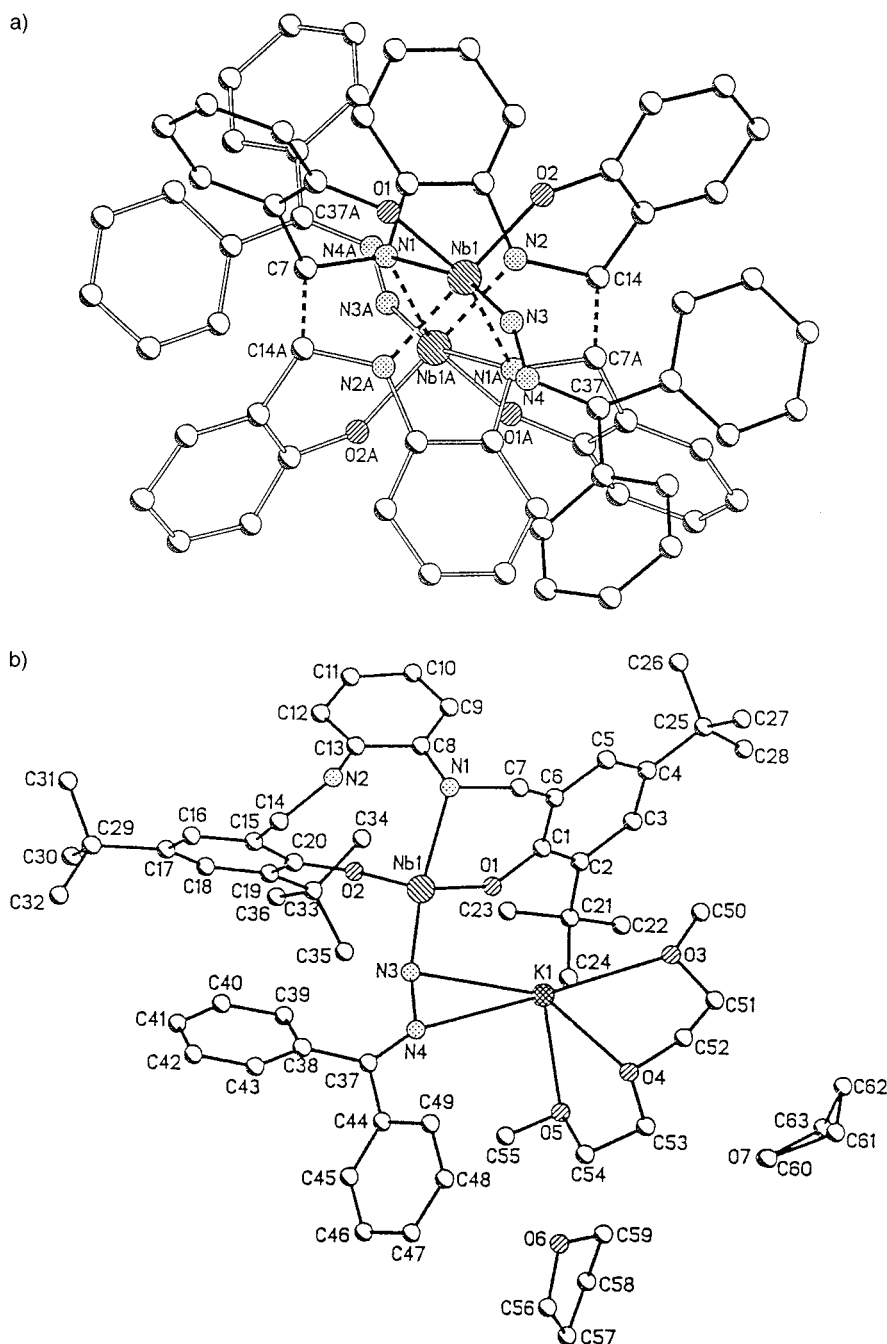


Figure 5. a) Structure of **6** (hydrogen atoms, $K(DME)^+$, solvent molecules and *t*Bu groups omitted for clarity). Atoms with an "A" indicate the following symmetry transformation: $-x, -y, -z$. b) A plot of complex **6** showing the asymmetric unit with the adopted labeling scheme (hydrogen atoms omitted for clarity).

bonds compared to the C–C bonds in the dinucleating structure.

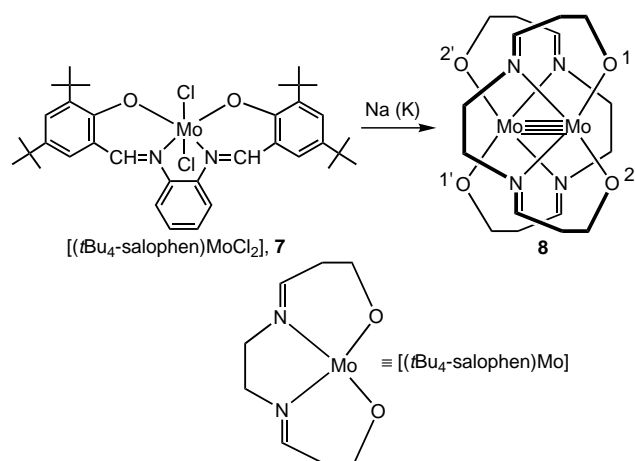
We then changed to another metal, molybdenum, coordinated to the same ligand, in order to explore further the competition in the formation and cleavage of the C–C and metal–metal bonds within the same structure, and to compare them with the theoretical forecast. To this purpose, we used as a model compound $[(tBu_4\text{-salophen})MoCl_2]$ (**7**, Scheme 3). Regardless of the Mo:reducing agent ratio, the reduction of **7** gives directly complex **8**, that contains a Mo–Mo quadruple bond and which seems to be the thermodynamic sink of the reaction. In this case, the experimental

results were completely in agreement with the theoretical forecast. Further reduction of **8** was unsuccessful and we did not see any intra- or intermolecular coupling between the salophen units by the formation of a C–C bond. In addition, as expected, no relevant reactivity was found related to the electron richness of the Mo–Mo quadruple bond.^[4, 13] The structure of **8** is displayed in Figure 6. It contains two $[(tBu\text{-salophen})Mo]$ units joined by a metal–metal quadruple bond (Mo–Mo 2.2057(8) Å).^[13] The two metal atoms Mo1 and Mo2 are displaced by -0.4847 and 0.4856 Å from the respective N_2O_2 planes. The two salophen skeletons in **8** maintain the expected planarity, and they are nearly parallel, the dihedral angle being 8.4° . The two $[(tBu\text{-salophen})Mo]$ units are rotated with respect to each other by $\approx 90^\circ$, the O1–Mo1–Mo2–O3 torsional angle being -88.2° .

Theoretical studies: In order to make the calculations feasible, the salophen ligand in the metal Schiff base complexes was simplified: the aromatic rings were replaced by C=C bonds. The simplified ligand, shown in Scheme 4, will be called salophen' hereafter. The geometry of the model systems considered was fully optimised starting from parameters deduced from the available experimental X-ray structures. We considered C_{2h} symmetry for $[M(\text{salophen}')_2]$ complexes and C_i symmetry for $[M_2(*\text{salophen}'_2*)]$

complexes, where $*\text{salophen}'_2*$ (Scheme 4) is the octadentate, octaanionic ligand derived by a four-electron reduction of two salophen' ligands.

The optimised structure of $[Mo(\text{salophen}')_2]$ is shown in Figure 7a. The calculated Mo–Mo bond length, 2.195 Å, is in very good agreement with the experimental value of 2.2057 Å and is typical of a Mo–Mo quadruple bond,^[3, 13] that is expected for a Mo^{II} complex. A metal-to-ligand four-electron transfer in the Mo^{II} complex $[Mo(\text{salophen}')_2]$ would give rise to the Mo^{IV} complex $[Mo_2(*\text{salophen}'_2*)]$, whose optimised geometry is shown in Figure 7b. The computed Mo–Mo bond length of 2.538 Å is very close to the experimental value of



Scheme 3. Reduction of 7 to give complex 8.

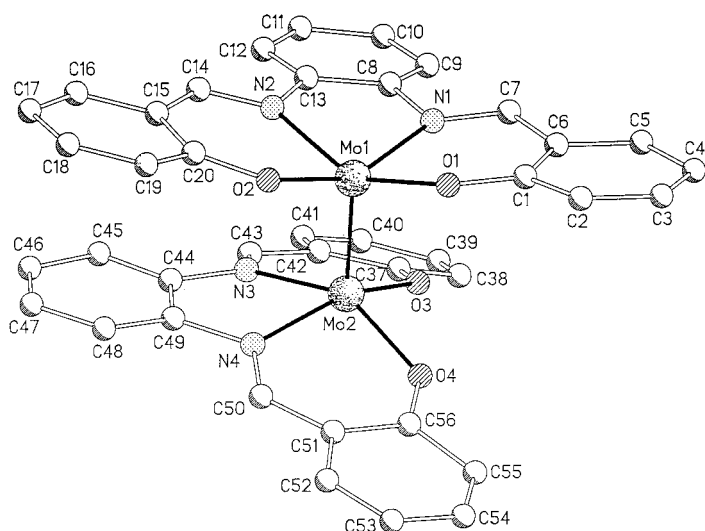
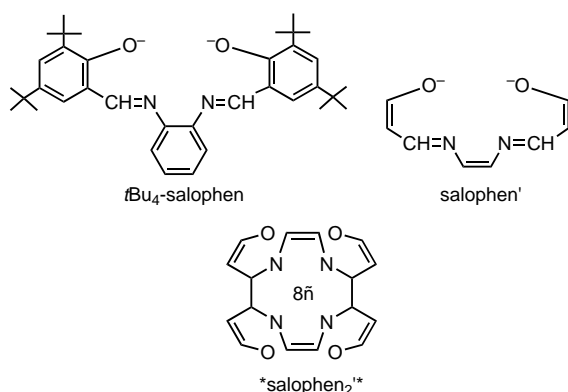
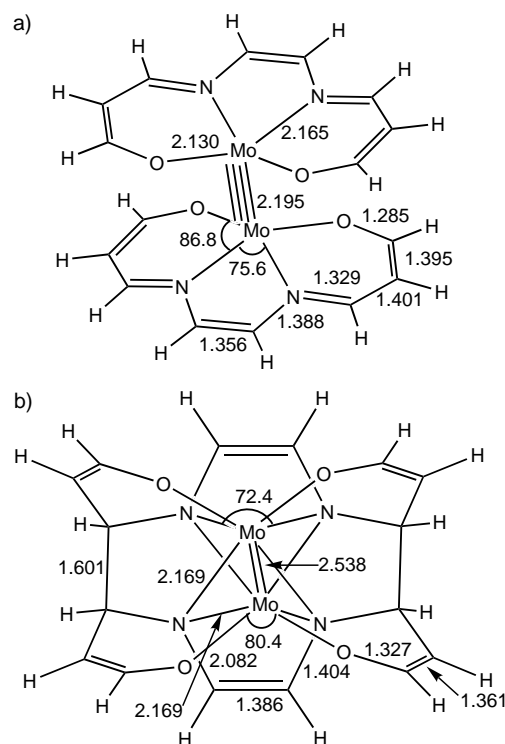


Figure 6. Structure of 8 with the adopted labeling scheme (hydrogen atoms and external solvent molecules omitted for clarity).



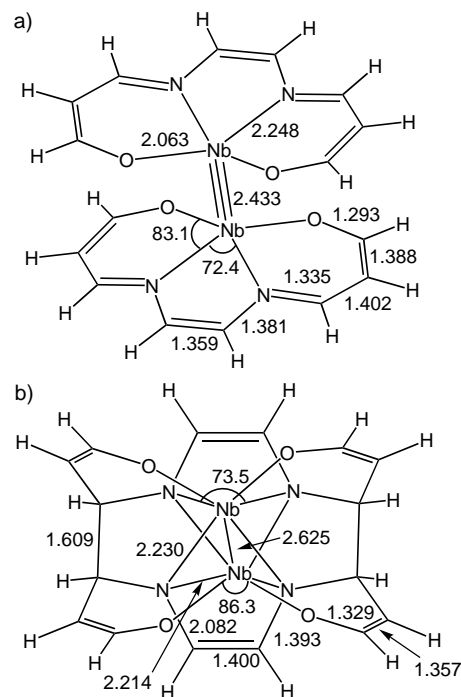
Scheme 4. Model representation of the salophen ligands used in the calculations.

2.544 Å found for a Mo–Mo double bond.^[3, 14] Figure 7b shows the presence of two C–C σ bonds ($r(\text{C}–\text{C}) = 1.601$ Å) between carbon atoms of the imino groups of the two salophen' ligands. $[\text{Mo}_2(*\text{salophen}'_2*)]$ is computed to be less stable than $[\text{Mo}(\text{salophen}')_2]$ by 70.5 kcal mol⁻¹, in agreement

Figure 7. Optimised structures of $[\text{Mo}(\text{salophen}')_2]$ (a) and $[\text{Mo}_2(*\text{salophen}'_2*)]$ (b) with selected bond lengths [Å] and angles [°].

with the experimental evidence that only species related to $[\text{Mo}(\text{salophen}')_2]$ can be synthesised.

Figure 8a shows the optimised structure of $[\text{Nb}(\text{salophen}')_2]$. The calculated Nb–Nb bond length, 2.433 Å, is typical of an Nb–Nb triple bond, as expected for an Nb^{II}

Figure 8. Optimised structures of $[\text{Nb}(\text{salophen}')_2]$ (a) and $[\text{Nb}_2(*\text{salophen}'_2*)]$ (b) with selected bond lengths [Å] and angles [°].

complex. A metal-to-ligand four-electron transfer in the Nb^{II} complex $[\text{Nb}(\text{salophen}')_2]$ would give rise to the Nb^{IV} complex $[\text{Nb}_2(*\text{salophen}'_2*)]$, whose optimised geometry is shown in Figure 8b. The computed Nb–Nb bond length of 2.625 Å is very close to the experimental value of 2.6528 Å found in the isolated system and is typical of a Nb–Nb single bond. Figure 8b shows the presence of two C–C σ bonds ($r(\text{C–C}) = 1.609$ Å) between carbon atoms of imino groups of the two salophen' ligands. This value is slightly shorter than the experimental value of 1.6281 Å. $[\text{Nb}_2(*\text{salophen}'_2*)]$ is computed to be less stable than $[\text{Nb}(\text{salophen}')_2]$ by only 12.5 kcal mol⁻¹. Considering that we analysed simplified model systems, this result is not in disagreement with the experimental evidence that only species related to $[\text{Nb}_2(*\text{salophen}'_2*)]$ can be synthesised and suggests that the species $[\text{Nb}_2(*\text{salophen}'_2*)]$ can be easily stabilised.

Figure 9 shows the analysis of the molecular orbitals of $[\text{Nb}_2(*\text{salophen}'_2*)]$. The frontier orbitals are mainly niobium in character, but the metal d orbitals are strongly mixed and a classification of these orbitals is not completely unambiguous.

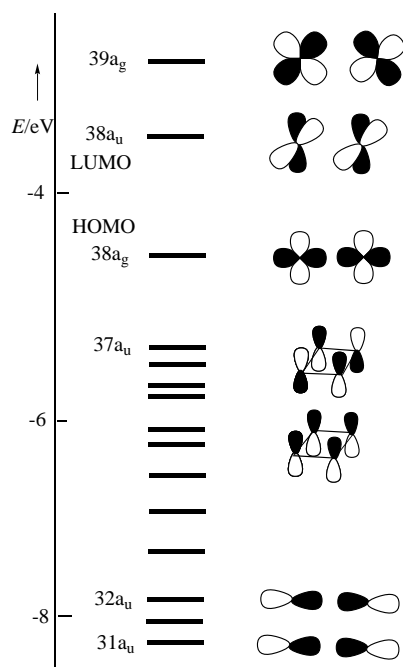


Figure 9. Frontier orbitals of $[\text{Nb}_2(*\text{salophen}'_2*)]$.

However, the highest occupied molecular orbital (HOMO), 38a_g, essentially describes a Nb–Nb σ bond, while the lowest unoccupied molecular orbital (LUMO), 38a_u, can be mainly characterised as a bonding δ orbital. The 39a_g orbital has mainly Nb–Nb π bonding character. The next valence orbitals at lower energies with respect to the HOMO are mainly composed of nitrogen *p* orbitals or other ligand atoms orbitals, while the orbitals 32a_u and 31a_u, that describe the two C–C σ bonds between carbon atoms of imino groups of the two salophen' ligands, lie at lower energies. An oxidation of $[\text{Nb}_2(*\text{salophen}'_2*)]$, therefore, should affect only the Nb–Nb bond and not the two C–C σ bonds. This is confirmed by the analysis of $[\text{Nb}_2(*\text{salophen}'_2*)]^{2+}$, whose optimised geometry

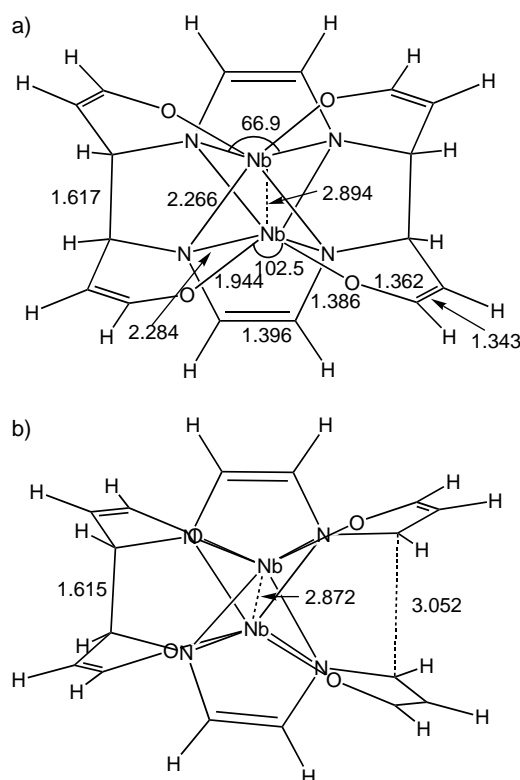
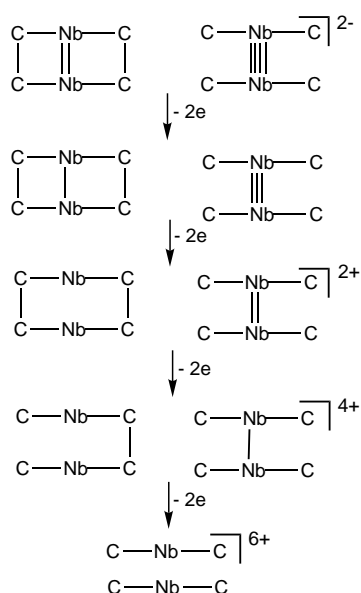


Figure 10. Optimised structures of $[\text{Nb}_2(*\text{salophen}'_2*)]^{2+}$ (a) and $[\text{Nb}_2(*\text{salophen}'_2*)]^{4+}$ (b) with selected bond lengths [Å] and angles [°].

is shown in Figure 10a. The computed Nb–Nb separation of 2.894 Å suggests a lack of any metal–metal interaction, while the C–C bond length of 1.617 Å confirms the presence of a bond between the carbon atoms of the imino groups of the two salophen' ligands.

Both $[\text{Nb}_2(*\text{salophen}'_2*)]$ and $[\text{Nb}(\text{salophen}')_2]$ can formally give rise to different levels of electron storage. The electron reservoirs are the C–C σ bonds between the carbon atoms of the imino groups of the two salophen' ligands or the metal–metal bonds in the $[\text{Nb}_2(*\text{salophen}'_2*)]$ species, while only metal–metal bonds can act as electron reservoirs in $[\text{Nb}(\text{salophen}')_2]$ complexes. In order to analyze this point we investigated, in addition to the neutral species, the 2–, 2+, 4+ and 6+ species. These species allow the storage or release of up to eight electrons (Scheme 5). The total energies and the main geometrical parameters of the investigated species are reported in Table 3. The optimised geometry of $[\text{Nb}_2(*\text{salophen}'_2*)]^{2-}$ shows two C–C σ bonds between the carbon atoms of the imino groups of the two salophen' ligands ($r(\text{C–C}) = 1.616$ Å) and an Nb–Nb bond length of 2.633 Å, a value very close to that found for the Nb–Nb single bond of the neutral complex.^[3] However, the analysis of the molecular orbitals reveals the presence of both a σ and a δ bond between the two metal centres. As expected, the δ bonding has a very small influence on the metal–metal separation.^[3] The neutral compound $[\text{Nb}_2(*\text{salophen}'_2*)]$ has already been discussed and shows a single Nb–Nb bond and two C–C σ bonds. A two-electron oxidation of this species, which produces $[\text{Nb}_2(*\text{salophen}'_2*)]^{2+}$, implies the cleavage of the Nb–Nb bond, as suggested by the Nb–Nb distance of 2.894 Å. The



Scheme 5. Different levels of electron storage.

Table 3. Total energies [Hartree], energy differences Δ [kcalmol⁻¹] and main geometrical parameters [Å] of the investigated niobium complexes.

Species ^[a]	Total energy	Δ	$r(\text{Nb-Nb})$	$r(\text{C-C})$
[Nb ₂ (*salophen ₂ *)] ²⁻	-10.064691		2.633	1.616
[Nb(salophen')] ₂ ²⁻	-10.124903	37.8	2.487	
[Nb ₂ (*salophen ₂ *)]	-10.129540		2.625	1.609
[Nb(salophen')] ₂	-10.149441	12.5	2.433	
[Nb ₂ (*salophen ₂ *)] ²⁺	-9.561418		2.894	1.617
[Nb(salophen')] ₂ ²⁺	-9.609573	30.2	2.680	
[Nb ₂ (*salophen ₂ *)] ⁴⁺	-8.406983		2.872	1.615 3.052
[Nb(salophen')] ₂ ⁴⁺	-8.488037	50.9	2.659	
[Nb ₂ (*salophen ₂ *)] ⁶⁺	-6.638021		2.851	1.796
[Nb(salophen')] ₂ ⁶⁺	-6.886307	155.8	3.011	

[a] Salophen' and *salophen₂*: see Scheme 4.

removal of another two electrons implies the breaking of one C–C σ bond. Indeed, in [Nb₂(*salophen'₂*)]⁴⁺, whose optimised structure is shown in Figure 10b, the distances between the carbon atoms of the imino groups are 1.615 Å and 3.052 Å: the first value corresponds to a σ bond, while the second one suggests the lack of any interaction. The removal of the next two electrons gives rise to two units which do not interact at all. As expected, the species [Nb₂(*salophen'₂*)]⁶⁺ is strongly destabilised. With regard to the [Nb(salophen')]₂^x species (where $x = 2-, 0, 2+, 4+, 6+$), we notice that we have a Nb–Nb quadruple bond in the dianion, a triple bond in the neutral species, a double bond in the dication, a single bond in the 4+ species and a lack of any metal–metal interaction in the 6+ species. [Nb(salophen')]₂⁶⁺ is essentially formed by two [Nb(salophen')]³⁺ units which do not interact at all. The optimised metal–metal bond lengths reported in Table 3 are in agreement with the observed progressive filling of metal–metal bonding orbitals: σ ; δ ; π ; δ . From the data of Table 3, we also notice that in the two analysed series of compounds, the metal–metal bonds are always preferred with respect to carbon–carbon bonds: the energy difference is small in the neutral compounds, while it is very high in the 6+ species.

Experimental Section

General procedure: All reactions were carried out under an atmosphere of purified nitrogen. Solvents were dried and distilled before use by standard methods.^[15] IR and NMR spectra were recorded respectively on Perkin-Elmer FT1600 spectrophotometer and on AC-200 or DPX-400 Bruker spectrometers. Ph₂CN₂^[16] and [Mo(*t*Bu₄-salophen)Cl₂] (7)^[9] were prepared according to published procedures.

Computational and methodological details: Density functional theory (DFT), which has been found to be a very cost-effective method to study transition metal systems,^[17] was used for the determination of equilibrium geometries and the evaluation of the energetics of all the investigated systems. All calculations were carried out with the Amsterdam density functional (ADF) program package.^[18, 19] Molecular structures were optimised at the non-local density approximation level of theory, in which the Becke non-local exchange^[20] and Perdew correlation^[21] corrections are included. The basis set employed for molybdenum and niobium was the uncontracted double- ζ quality for 4s and 4p, triple- ζ quality for 4d and 5s, augmented by two 5p functions. The main-group elements were described by a double- ζ basis augmented by one 2p function for hydrogen and one 3d polarisation function for the other elements. The cores (Mo, Nb: 1s-3d; C, N, O: 1s) were kept frozen.^[22]

Synthesis of 1: NbCl₅ (17.43 g, 64.5 mmol) was dissolved in toluene (500 mL) and the red solution was stirred overnight. *t*Bu₄-salophenH₂ (34.92 g; 64.5 mmol) was added to give a red suspension that was refluxed for 24 h. Toluene was evaporated and the solid was washed with diethyl ether (2 × 250 mL), collected and dried in vacuo (45 g, 84%). ¹H NMR (200 MHz, [D₆]DMSO, 298 K): $\delta = 9.15$ (s, 1H; CH=N), 7.82 (m, 2H; tol), 7.67 (d, $J = 2.4$ Hz, 1H; Ar), 7.56 (d, $J = 2.4$ Hz, 1H; Ar), 7.48 (m, 2H; tol), 7.16 (m, 3H; Ar+tol), 2.28 (s, 3H; tol), 1.42 (s, 9H; CH₃), 1.27 (s, 9H; CH₃); elemental analysis calcd (%) for C₄₃H₅₄Cl₃N₂NbO₂ (830.2): C 62.21, H 6.56, N 3.37; found: C 61.88, H 6.53, N 3.41.

Synthesis of 2: Magnesium turnings (0.24 g, 9.9 mmol) were added to a solution of **1** (5.48 g; 6.6 mmol) in THF (100 mL). The resulting dark-red suspension was stirred for 6 d. A yellow-green solid was collected by filtration and dried in vacuo (4.6 g, 61%). ¹H NMR (400 MHz, [D₃]pyridine, 323 K): $\delta = 7.65$ (d, $J = 2.5$ Hz, 1H; Ar), 7.41 (d, $J = 2.5$ Hz, 1H; Ar), 6.19 (m, 1H; Ar), 5.88 (m, 1H; Ar), 5.50 (s, 1H; CHN), 3.65 (m, 4H; THF), 1.63 (m, 4H; THF), 1.43 (s, 9H; CH₃), 1.42 (s, 9H; CH₃); elemental analysis calcd (%) for C₄₀H₅₄N₂NbO₃ (703.8): C 68.26, H 7.73, N 3.98; found: C 67.79, H 7.91, N 3.95. Crystals suitable for X-ray analysis were grown by slowly cooling a hot saturated THF solution to room temperature.

Synthesis of 3: A solution of I₂ (90 mg, 0.36 mmol) in CH₂Cl₂ (20 mL) was added to a yellow-green solution of **2** (0.50 g; 0.36 mmol) in CH₂Cl₂ (100 mL) which had been previously cooled and maintained at -30 °C. The mixture was allowed to reach room temperature before the solution was dried. The dark green residue was then suspended in *n*-hexane (90 mL), collected and dried in vacuo (0.44 g, 81%). ¹H NMR (400 MHz, CD₂Cl₂, 298 K): $\delta = 7.45$ (d, $J = 2.6$ Hz, 1H; Ar), 7.19 (d, $J = 2.6$ Hz, 1H; Ar), 6.63 (m, 1H; Ar), 6.38 (m, 1H; Ar), 4.82 (s, 1H; CH-N), 1.39 (s, 9H; CH₃), 1.36 (s, 9H; CH₃); elemental analysis calcd (%) for C₃₆H₄₆IN₂NbO₂ (758.6): C 57.00, H 6.11, N 3.69; found: C 56.78, H 5.89, N 3.48.

Synthesis of 4: AgSO₃CF₃ (300 mg; 1.15 mmol) was added to a yellow-green suspension of **2** (0.81 g, 0.58 mmol) in CH₂Cl₂ (110 mL). The mixture was refluxed overnight to afford a deep green suspension. Ag metal was filtered off and the solution evaporated to dryness. The dark green residue was suspended in hexane (90 mL), collected and dried in vacuo (0.66 g, 73%). ¹H NMR (400 MHz, CD₂Cl₂, 298 K): $\delta = 7.49$ (d, $J = 2.5$ Hz, 1H; Ar), 7.46 (d, $J = 2.5$ Hz, 1H; Ar), 7.21 (d, $J = 2.5$ Hz, 1H; Ar), 7.14 (d, $J = 2.5$ Hz, 1H; Ar), 6.87 (m, 1H; Ar), 6.78 (m, 1H; Ar), 6.64 (m, 1H; Ar), 6.37 (m, 1H; Ar), 5.37 (d, $J = 1.8$ Hz, 1H; CH-N), 5.03 (d, $J = 1.8$ Hz, 1H; CH-N), 1.39 (s, 9H; CH₃), 1.36 (s, 9H; CH₃), 1.33 (s, 9H; CH₃), 1.30 (s, 9H; CH₃); elemental analysis calcd (%) for C₃₇H₄₆F₃N₂NbO₅S (780.8): C 56.92, H 5.94, N 3.59; found: C 55.78, H 6.41, N 3.29. Crystals suitable for X-ray analysis were grown by slowly cooling a pyridine/diethyl ether solution to 4 °C.

Synthesis of 6: Ph₂CN₂ (0.52 g, 2.7 mmol) was added to a yellow-green suspension of **2** (1.9 g; 1.35 mmol) in THF (60 mL) to give a red solution that was cooled to -80 °C. A deep green THF (60 mL) solution containing K and naphthalene in an equimolar amount (2.7 mmol) was added. The

resulting mixture was stirred for 30 min at -80°C and then allowed to warm slowly to room temperature. The red solution was concentrated to 40 mL and *n*-hexane (100 mL) was added. A red solid precipitated which was collected and dried in vacuo (1.7 g, 58%). ^1H NMR (400 MHz, $[\text{D}_5]$ pyridine, 300 K): $\delta = 8.14$ (d, $J = 7.5$ Hz, 1H; Ph), 8.00 (d, $J = 7.5$ Hz, 1H; Ph), 7.57 (d, $J = 2.7$ Hz, 1H; Ar), 7.52 (d, $J = 2.7$ Hz, 1H; Ar), 7.48 (d, $J = 8$ Hz, 1H; Ph), 7.36 (m, 1H; Ph), 7.24 (t, $J = 8$ Hz, 1H; Ph), 7.16 (d, $J = 2.7$ Hz, 1H; Ar), 7.10 (m, 2H; Ph), 7.04 (d, $J = 2.7$ Hz, 1H; Ar), 6.99 (m, 2H; Ph), 6.79 (m, 1H; Ph), 6.34 (m, 1H; Ar), 6.30 (m, 1H; Ar), 6.17 (m, 1H; Ar), 6.11 (m, 1H; Ar), 5.58 (d, $J = 1.7$ Hz, 1H; CH-N), 4.39 (d, $J = 1.7$ Hz, 1H; CH-N), 3.67 (m, 12H; thf), 1.67 (m, 12H; thf), 1.70 (s, 9H; CH_3), 1.58 (s, 9H; CH_3), 1.55 (s, 9H; CH_3), 1.50 (s, 9H; CH_3); elemental analysis calcd (%) for $\text{C}_{61}\text{H}_{80}\text{KN}_4\text{NbO}_5$ (1081.3): C 67.76, H 7.46, N 5.18; found: C 67.85, H 7.03, N 5.60. Crystals suitable for X-ray analysis were grown by slowly cooling a diglyme/diethyl ether solution to 4°C .

Synthesis of 8: Sodium (0.43 g, 18.7 mmol) and naphthalene (0.2 g, 1.5 mmol) were added to a suspension of **7** (6.58 g; 9.33 mmol) in THF (250 mL). The resulting black suspension was stirred for 6 d, then NaCl was filtered off. The solution was evaporated to dryness. The residue was suspended in pentane, collected by filtration and dried in vacuo (2.2 g, 74%). IR (Nujol): $\bar{\nu} = 1599$ (m), 1571 (m), 1529 (s), 1424 (m), 1297 (w), 1266 (s), 1196 (m), 1180 (m), 1030 (w), 840 (s), 745 (s), 700 (s), 573 (w) cm^{-1} ; elemental analysis calcd (%) for $\text{C}_{36}\text{H}_{46}\text{MoN}_2\text{O}_2$ (634.7): C 68.12, H 7.30, N 4.41; found: C 67.98, H 7.45, N 4.21. Crystals suitable for X-ray analysis were grown at room temperature from a pentane/*n*-heptane (1:1) solution.

X-ray crystallography for complexes 2, 4, 6 and 8: The relevant details of the crystals, data collection and structure refinement are listed in Table 1. Diffraction data were collected at 143 K on different equipment: mar345 imaging plate detector (**6**), Kuma diffractometer with a kappa geometry and equipped with a Sapphire CCD detector (**2, 8**), or a Rigaku AFC7S diffractometer equipped with a Mercury CCD (**4**). Data reduction was performed, respectively, with marHKL release 1.9.1,^[23] CrsAlis RED 1.6.7^[24] and Crystal Clear 1.2.2.^[25] Absorption correction^[26] was applied to one data set (**4**). Structure solutions were determined with ab initio direct methods.^[27] All structures were refined using the full-matrix least-squares on F^2 with all non-H atoms anisotropically defined. H atoms were placed in calculated positions with the "riding model" with $U_{\text{iso}} = a^*U_{\text{eq}}(\text{C})$ (where a is 1.5 for methyl hydrogen atoms and 1.2 for others, C is the parent carbon atom). Some disorder problems were encountered during the refinement of **4** and **8** (CF_3SO_3^- showing high vibrational motion or disordered *t*Bu substituents, respectively). Structure refinement, molecular graphics and geometrical calculation were carried out on all structures with the SHELXTL software package, release 5.1.^[28] Crystallographic data (excluding structure factors) for the structures reported in this paper have been deposited with the Cambridge Crystallographic Data Centre as supplementary publication nos. CCDC-156320 (**2**), CCDC-156321 (**4**), CCDC-156322 (**6**) and CCDC-156323 (**8**). Copies of the data can be obtained free of charge on application to CCDC, 12 Union Road, Cambridge CB21EZ, UK (fax: (+44) 1223-336-033; e-mail: deposit@ccdc.cam.ac.uk).

Acknowledgements

We thank the "Fonds National Suisse de la Recherche Scientifique" (Bern, Switzerland, Grant No. 20-61'246.00); Action COSTD9 (European Program for Scientific Research, OFES No. C98.008) and Fondation Herbette (University of Lausanne, N.R.) for financial support.

- [1] For a recent exhaustive review on electron transfer, bond breaking and bond formation see: J.-M. Savéant in *Advances in Physical Organic Chemistry*, Vol. 35 (Ed.: T. T. Tidwell), Academic Press, San Diego, **2000**, pp. 117–192.
- [2] a) J. Mathieu, J. Weill-Raynal, *Formation of C–C Bonds*, Thieme, Stuttgart, **1973**; b) *Carbon–Carbon Bond Formation Using Organometallic Compounds* (Eds.: F. R. Hartley, S. Patai), Wiley, Chichester, **1985**; c) G. M. Robertson in *Comprehensive Organic Synthesis*, Vol. 3 (Eds.: B. M. Trost, I. Fleming), Pergamon, Oxford, **1991**, Chapt. 2.6; d) A. Armstrong in *Comprehensive Organic Functional Group Transformations*, Vol. 1 (Eds.: A. R. Katritzky, O. Meth-Cohn, C. W. Rees), Pergamon, Oxford, **1995**, Chapt. 1.07.
- [3] a) F. A. Cotton, R. A. Walton, *Multiple Bonds Between Metal Atoms*, 2nd ed., Oxford University Press, New York, **1993**; b) F. A. Cotton, G. Wilkinson, C. A. Murillo, M. Bochmann, *Advanced Inorganic Chemistry*, 6th ed., Wiley, New York, **1999**, pp. 957–962, and references therein.
- [4] a) L. A. Fluharty in *The Chemistry of the Thiol Group* (Ed.: S. Patai), Wiley, London, **1974**, Chapt. 13; b) R. Singh, G. M. Whitesides in *Supplement S: The Chemistry of Sulfur-Containing Functional Groups* (Eds.: S. Patai, Z. Rappoport), Wiley, Chichester, **1993**, Chapt. 13.
- [5] a) R. J. Simmons, *Chemistry of Biomolecules: an Introduction*, Royal Society of Chemistry, Cambridge, **1992**, Chapt. 10; b) B. Testa, *Biochemistry of Redox Reactions*, Academic Press, London, **1995**, Chapt. 10; c) M. M. Bloomfield, L. J. Stephens, *Chemistry and the Living Organism*, 6th ed., Wiley, New York, **1996**; Chapt. 17; d) *Protein Structure: a Practical Approach*, 2nd ed. (Ed.: T. E. Creighton), Oxford University Press, New York, **1997**.
- [6] a) H. Wadeppohl, S. Gebert, H. Pritzkow, D. Osella, C. Nervi, J. Fiedler, *Eur. J. Inorg. Chem.* **2000**, 1833–1843; b) A. K. Ghosh, K. N. Mitra, G. Mostafa, S. Goswami, *Eur. J. Inorg. Chem.* **2000**, 1961–1967; c) M.-H. Baik, T. Ziegler, C. K. Schauer, *J. Am. Chem. Soc.* **2000**, *122*, 9143–9154, and references therein.
- [7] R. Rathore, P. Le Magueres, S. V. Lindeman, J. K. Kochi, *Angew. Chem.* **2000**, *112*, 818–821; *Angew. Chem. Int. Ed.* **2000**, *39*, 809–812, and references therein.
- [8] R. Rathore, J. K. Kochi in *Advances in Physical Organic Chemistry*, Vol. 35 (Ed.: T. T. Tidwell), Academic Press, San Diego, **2000**, pp. 192–318, and references therein.
- [9] a) S. De Angelis, E. Solari, E. Gallo, C. Floriani, A. Chiesi-Villa, C. Rizzoli, *Inorg. Chem.* **1996**, *35*, 5995–6003; b) E. Gallo, E. Solari, N. Re, C. Floriani, A. Chiesi-Villa, C. Rizzoli, *J. Am. Chem. Soc.* **1997**, *119*, 5144–5154; c) E. Solari, C. Maltese, F. Franceschi, C. Floriani, A. Chiesi-Villa, C. Rizzoli, *J. Chem. Soc. Dalton Trans.* **1997**, 2903–2910; d) F. Franceschi, E. Solari, C. Floriani, A. Chiesi-Villa, C. Rizzoli, M. Rosi, *Chem. Eur. J.* **1999**, *5*, 708–721; e) F. Franceschi, E. Solari, R. Scopelliti, C. Floriani, *Angew. Chem.* **2000**, *112*, 1751–1753; *Angew. Chem. Int. Ed.* **2000**, *39*, 1685–1689; f) E. Solari, C. Maltese, M. Latronico, C. Floriani, A. Chiesi-Villa, C. Rizzoli, *J. Chem. Soc. Dalton Trans.* **1998**, 2395–2400.
- [10] F. Franceschi, J. Hesschenbrouk, E. Solari, C. Floriani, N. Re, A. Chiesi-Villa, C. Rizzoli, *J. Chem. Soc. Dalton Trans.* **2000**, 593–604.
- [11] M. Rosi, A. Sgamellotti, F. Franceschi, C. Floriani, *Chem. Eur. J.* **1999**, *5*, 2914–2920.
- [12] a) A. Caselli, E. Solari, R. Scopelliti, C. Floriani, *J. Am. Chem. Soc.* **1999**, *121*, 8296–8305; b) C. Floriani, *Chem. Eur. J.* **1999**, *5*, 19–23; c) A. Caselli, E. Solari, R. Scopelliti, C. Floriani, *J. Am. Chem. Soc.* **2000**, *122*, 538–539; d) A. Caselli, E. Solari, R. Scopelliti, C. Floriani, N. Re, C. Rizzoli, A. Chiesi-Villa, *J. Am. Chem. Soc.* **2000**, *122*, 3652–3670.
- [13] G. Pennesi, C. Floriani, A. Chiesi-Villa, C. Guastini, *J. Chem. Soc. Chem. Commun.* **1988**, 350–351.
- [14] a) M. H. Chisholm, C. E. Hammond, J. C. Huffman, *Polyhedron* **1989**, *8*, 129–131; b) H. E. King, Jr., L. A. Mundi, K. G. Strohmaier, R. C. Haushalter, *J. Solid State Chem.* **1991**, *92*, 1–7.
- [15] W. L. F. Armarego, D. D. Perrin, *Purification of Laboratory Chemicals*, 4th ed., Butterworth-Heinemann, Oxford, **1996**.
- [16] L. I. Smith, K. L. Howard, *Org. Synth. Coll. Vol. 3* **1955**, 351–352.
- [17] See, for example: C. W. Bauschlicher, A. Ricca, H. Partridge, S. R. Langhoff, in *Recent Advances in Density Functional Theory* (Ed.: D. P. Chong), World Scientific Publishing Co. (Singapore), **1997**, Part II.
- [18] ADF 1999, E. J. Baerends, A. Bérces, C. Bo, P. M. Boerrigter, L. Cavallo, L. Deng, R. M. Dickson, D. E. Ellis, L. Fan, T. H. Fischer, C. Fonseca Guerra, S. J. A. van Gisbergen, J. A. Groeneveld, O. V. Gritsenko, F. E. Harris, P. van den Hoek, H. Jacobsen, G. van Kessel, F. Kootstra, E. van Lenthe, V. P. Osinga, P. H. T. Philipsen, D. Post, C. C. Pye, W. Ravenek, P. Ros, P. R. T. Schipper, G. Schreckenbach, J. G. Snijders, M. Sola, D. Swerhone, G. te Velde, P. Vernooijs, L. Versluis, O. Visser, E. van Wezenbeek, G. Wiesenekker, S. K. Wolff, T. K. Woo, T. Ziegler.
- [19] C. Fonseca Guerra, J. G. Snijders, G. te Velde, E. J. Baerends, *Theor. Chem. Acc.* **1998**, *99*, 391–403.
- [20] A. D. Becke, *Phys. Rev. A* **1988**, *38*, 3098–3100.

- [21] a) J. P. Perdew, *Phys. Rev. B* **1986**, 33, 8822–8824; b) J. P. Perdew, *Phys. Rev. B* **1986**, 34, 7406 (erratum).
- [22] a) E. J. Baerends, D. E. Ellis, P. Ros, *Chem. Phys.* **1973**, 2, 41–51; b) E. J. Baerends, P. Ros, *Chem. Phys.* **1973**, 2, 52–59; c) **1975**, 8, 412–418; d) E. J. Baerends, P. Ros, *Int. J. Quantum Chem., Quantum Chem. Symp.* **1978**, 12, 169–190.
- [23] Z. Otwinowski, W. Minor in *Methods in Enzymology*, Vol. 276: *Macromolecular Crystallography* (Eds.: C. W. Carter Jr., R. M. Sweet), Academic Press, San Diego, **1997**, part A, 307–326.
- [24] Kuma Diffraction Instruments GmbH, PSE-EPFL module 3.4, CH-1015 Lausanne (Switzerland), **2000**.
- [25] J. W. Pflugrath, *Acta Crystallogr. Sect. D* **1999**, 55, 1718–1725.
- [26] teXsan for Windows 1.0.6 and REQAB4 1.1 (Molecular Structure Corporation, New Trails Drive, The Woodlands, Texas, 77381–5209, USA, **1997–1999**).
- [27] G. M. Sheldrick, *Acta Crystallogr. Sect. A* **1990**, 46, 467–473.
- [28] Bruker AXS, Inc., Madison, Wisconsin, 53719, USA, **1997**.

Received: January 22, 2001 [F3019]